ELSEVIER

Polymer 43 (2002) 2495–2500

polymer

www.elsevier.com/locate/polymer

Microstructure, tensile properties, and biodegradability of aliphatic polyester/clay nanocomposites

Sang-Rock Lee[a], Hwan-Man Park[a], Hyuntaek Lim[a], Taekyu Kang[a], Xiucuo Li[b], Won-Jei Cho[a], Chang-Sik Ha[a,*]

[a]*Department of Polymer Science and Engineering, Pusan National University, Pusan 609-735, South Korea*
[b]*School of Chemical Engineering, Hebei University of Technology, Tianjin 300130, People's Republic of China*

Received 16 August 2001; received in revised form 29 October 2001; accepted 26 November 2001

Abstract

Novel biodegradable aliphatic polyester (APES)/organoclay nanocomposites were prepared through melt intercalation method. Two kinds of organoclays, Cloisite 30B and Cloisite 10A with different ammonium cations located in the silicate gallery, were chosen for the nanocomposites preparation. The dispersion of the silicate layers in the APES hybrids was characterized by using X-ray diffraction (XRD) and transmission electron microscopy (TEM). Tensile properties and the biodegradability of the APES/organoclay nanocomposites were also studied. APES/Cloisite 30B hybrids showed higher degree of intercalation than APES/Cloisite 10A hybrids due to the strong hydrogen bonding interaction between APES and hydroxyl group in the gallery of Cloisite 30B silicate layers. This leads to higher tensile properties and lower biodegradability for APES/Cloisite 30B hybrids than for the APES/Cloisite 10A hybrids. © 2002 Elsevier Science Ltd. All rights reserved.

Keywords: Biodegradable; Nanocomposites; Aliphatic polyester

1. Introduction

Biodegradable polymers have been extensively investigated, since 1970s, in order to reduce the environmental pollution caused by plastic wastes [1,2]. Synthetic biodegradable aliphatic polyesters (APES), which are synthesized from diol and dicarboxylic acid through condensation polymerization, are known to be completely biodegradable in soil and water and to be one of the effective packing materials. Even though APES can compete in cost with bacterial APES such as poly (hydroxybutyrate) (PHB), it is still much more expensive and lacks mechanical strength compared with conventional plastics. If the properties of the APES can be further improved by the addition of a small quantity of an environmentally benign material, this polymer will find applications in more special or severe circumstances.

Melt intercalation of polymers into the layered silicates of clay has been proven to be an excellent technique to prepare polymer-layered silicate nanocomposites (PLS) [3–6]. With only a few percent of clay, PLS exhibits greatly improved mechanical, thermal and barrier properties compared with the pristine polymers [7]. More importantly, clay is environmentally friendly, naturally abundant and economic. To realize the combination of the biodegradability of APES with the high strength and stability of the clay, APES/organic clay nanocomposites were prepared through melt intercalation method in the present work.

So far there are no reports on the preparation of biodegradable PLS nanocomposites except poly (ϵ-caprolactone)/clay hybrids [8–10]. The objective of our research is to investigate the influence of the nanostructure on the tensile properties and the biodegradability of APES. In this paper, the APES/organoclay nanocomposites were prepared and characterized by X-ray diffraction (XRD) and transmission electron microscopy (TEM). The tensile and biodegradable properties were also measured.

2. Experimental

2.1. Materials

Biodegradable APES was kindly supplied by Sunkyong Co. Korea under the trade name of Skygreen-2109. It is a copolymer prepared by polycondensation of aliphatic glycols (ethylene glycol and 1,4-butanediol) and aliphatic

* Corresponding author. Tel.: +82-51-510-2407; fax: +82-51-514-4331.
E-mail address: csha@pnu.edu (C.-S. Ha).

0032-3861/02/$ - see front matter © 2002 Elsevier Science Ltd. All rights reserved.
PII: S0032-3861(02)00012-5

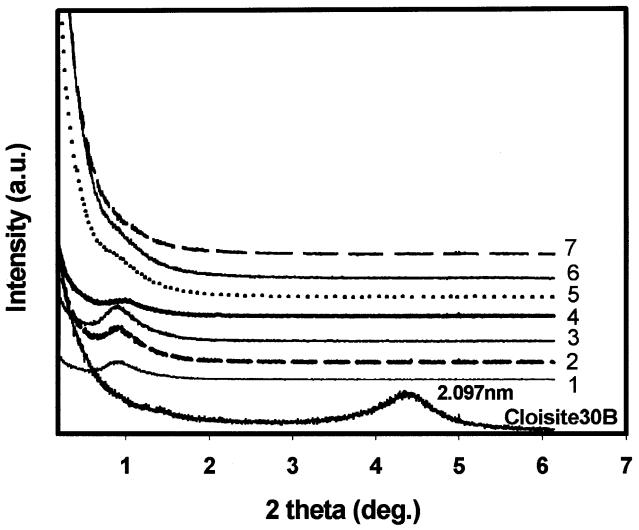

Fig. 1. XRD patterns of APES/Cloisite 30B hybrids with various contents of Cloisite 30B: (1) 1 wt%; (2) 3 wt%; (3) 5 wt%; (4) 10 wt%; (5) 15 wt%; (6) 20 wt%; (7) 30 wt%.

dicarboxylic acids (succinic acid and adipic acid) with weight-average molecular weight of 60,000. Two kinds of organically modified montmorillonite (MMT) (organoclay), Cloisite 30B and Cloisite 10A, were chosen in our experiments. They are products of Southern Clay Co., which contain different ammonium cations: methyl tallow bis-2-hydroxyethyl ammonium for Cloisite 30B and dimethyl benzyl hydrogenated-tallow ammonium for Cloisite 10A, respectively.

2.2. Preparation of APES/organoclay nanocomposites

Cloisite 30B, Cloisite 10A and APES were dried under vacuum at 80 °C for at least 24 h. Dried APES and organoclays were mixed in a Haake Rheocord mixer at 130 °C, 50 rpm for 30 min. The hybrids were then injection molded using a CS-183 MMX mini MAX molder (Custom Scientific Instruments, Inc.) at 130 °C to get dog-bone shaped specimens for characterization and tensile testing.

2.3. Characterization of the nanocomposites

Synchrotron XRD patterns were taken with a Rigaku X-ray generator operated at 40 kV and 40 mA in the Pohang Accelerator Laboratory, POSTECH, Korea. The scanning rate is 0.2 °/min. The basal spacing of the silicate layer, d, was calculated using the Bragg's equation, $\lambda = 2d \sin \theta$. TEM images were taken from cryogenically microtomed ultra thin sections using a Hitachi H-800 TEM.

2.4. Measurements

Viscosity measurements of hybrids were performed with the Rheometric Dynamic Analyser (Rheometrics Co., RDA II). Samples were molded into parallel plates of 25 mm(ϕ) × 2 mm dimension. The samples were subjected to a sinusoidal strain in the torsion mode. The percentage strain and the frequency during temperature sweep were 0.1% and 1 rad/s, respectively. The temperature was increased at the rate of 10 °C/min. Each sample was analyzed in duplicate. Tensile testing of the nanocomposites were carried out by an UTM (Universal Testing Machine) modeled UL25 (Hounsfield Co.) at room temperature. The crosshead speed was 10 mm/min. All measurements were performed for five replicates of dog-bone shaped specimens and averaged to get the final result.

To evaluate the biodegradability of the APES/organoclay hybrids, the specimens were hot pressed to get thin films of about 0.12 mm thickness. The films were buried in the activated soil, which consisted of 50 wt% of soil, 30 wt% of sand and 20 wt% of composted manure with pH 7.0 ± 0.5, and kept at the temperature of 60 °C and the relative humidity of 60 ± 5%. At predetermined intervals, the specimens were recovered from the soil, cleansed with 100, 50, 25 and 0% buffer/ethanol solution, and dried in a vacuum oven. The dried films were weighed to calculate the weight loss. An average of five measurements were taken.

3. Results and discussion

3.1. Characterization of the APES/organoclay nanocomposites

The XRD patterns of the mixtures of APES with various amounts of Cloisite 30B or Cloisite 10A are shown in Figs. 1 and 2, respectively. For APES/Cloisite 30B hybrids with the content of Cloisite 30B less than 15 wt%, the interlayer spacing has increased from 2.097 nm of the original Cloisite 30B to around 10 nm (2θ about 1°), indicating the great extent of intercalation of the Cloisite 30B layers by APES. While those containing higher amounts of Cloisite 30B showed almost no peaks, indicating an exfoliation of the Cloisite 30B in the APES matrix. For APES/Cloisite 10A hybrids with Cloisite 10A contents less than 15 wt%, two peaks exist corresponding to the interlayer spacing of 10 and 3.25 nm, much larger than that of the original Cloisite 10A (i.e. 1.092 nm). Almost the same trend appeared with increasing the amount of Cloisite 10A as that of Cloisite 30B, that is, the peaks nearly disappeared in the XRD patterns when the Cloisite 10A contents exceeded 15 wt%.

From the above results, it is clear that the intercalation extent of the Cloisite 30B by APES is greater than that of the Cloisite 10A. This is attributed to the strong interaction or miscibility between APES and Cloisite 30B which originates from the strong hydrogen bonding between the carboxyl group of APES and the hydroxyl group in the gallery of Cloisite 30B. The interaction between APES and Cloisite 10A is not as strong as that between APES and Cloisite 30B due to the weak polarity of ammonium cation in the Cloisite 10A gallery. Though APES can intercalate into the silicate layers of the Cloisite 10A, the degree

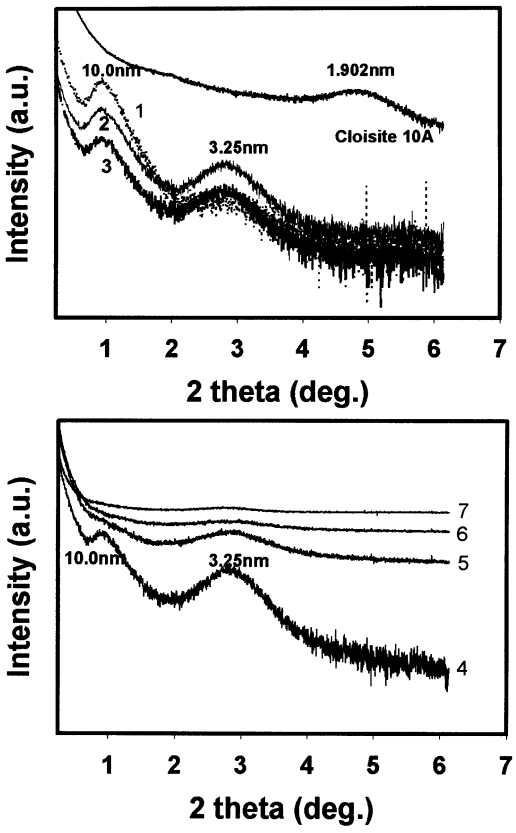

Fig. 2. XRD patterns of APES/Cloisite 10A hybrids with various contents of Cloisite 10A: (1) 1 wt%; (2) 3 wt%; (3) 5 wt%; (4) 10 wt%; (5) 15 wt%; (6) 20 wt%; (7) 30 wt%.

of intercalation is less at the same mixing conditions. Other researchers found similar results in polymer/clay nanocomposites preparation that strong polar-type interactions especially hydrogen bonding are critical for the formation of intercalated and especially exfoliated hybrids via polymer intercalation [11–13].

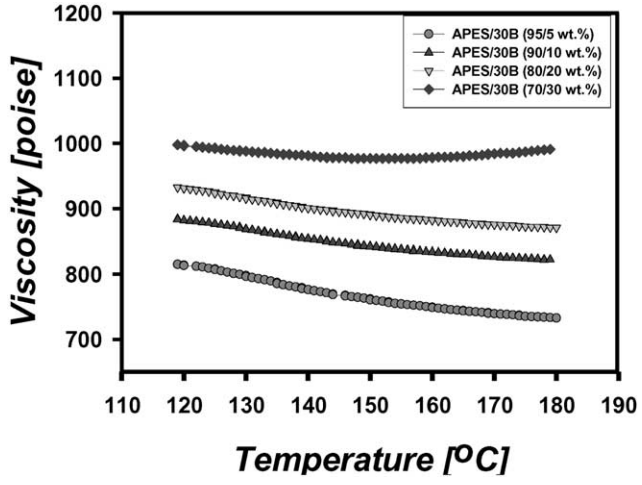

Fig. 3. Influence of the Cloisite 30B content on the viscosity against temperature behavior of APES/Cloisite 30B hybrids.

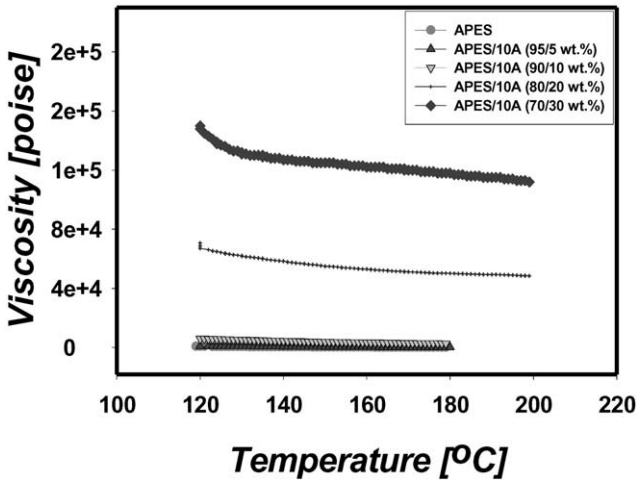

Fig. 4. Influence of the Cloisite 10A content on the viscosity against temperature behavior of APES/Cloisite 10A hybrids.

On the other hand, if the nanocomposite formation is thermodynamically favored, or in other words, the polymer and the organoclays are miscible or partially miscible, the dispersion of the clay in the polymer matrix will depend on the intercalation kinetics [14]. For example, the medium viscosity, the existence of shear, the mixing temperature and time may also influence the morphology of certain polymer/clay hybrids. Even though some polymers have been reported to form exfoliated nanocomposites with organoclay content as high as more than 20 wt% [9], the case is not always true since the existence of more amount of clay has the tendency to aggregate in the polymer matrix. Here the XRD patterns of APES/Cloisite 10A and APES/Cloisite 30B hybrids show no peaks at high contents of Cloisite 30B and Cloisite 10A, indicating the exfoliated structure, in contrast to the intercalated nanostructure at low organoclay contents. This is unusual and may be related in part to the effect of shear on the formation of polymer/clay nanocomposites via melt intercalation. Increase in the content of organoclays in the APES hybrids results in high melt viscosity as shown in Figs. 3 and 4, thus high shear force during mixing at constant rotor speed. The presence of the applied strong shear would promote the exfoliation of the silicate layers [14,15], at the same time, the optimum combination of the external shear and the suitable interaction between APES and Cloisite 30B or Cloisite 10A at proper mixing temperature and time should be responsible for the exfoliated nanocomposites [16]. More detailed investigation about the influence of shear on different polymer/clay hybrid formation kinetics is under way.

To further confirm the above results, TEM micrographs are presented in Figs. 5 and 6. The TEM images of the APES/Cloisite Cloisite 30B hybrids exhibit multilayer morphologies with alternating polymeric and inorganic silicate layers (Fig. 5a–c), and so does the APES/Cloisite Cloisite 10A hybrid (Fig. 6–c), respectively. The contents of the Cloisite clays in the polymer matrix are 5 and 10 wt%.

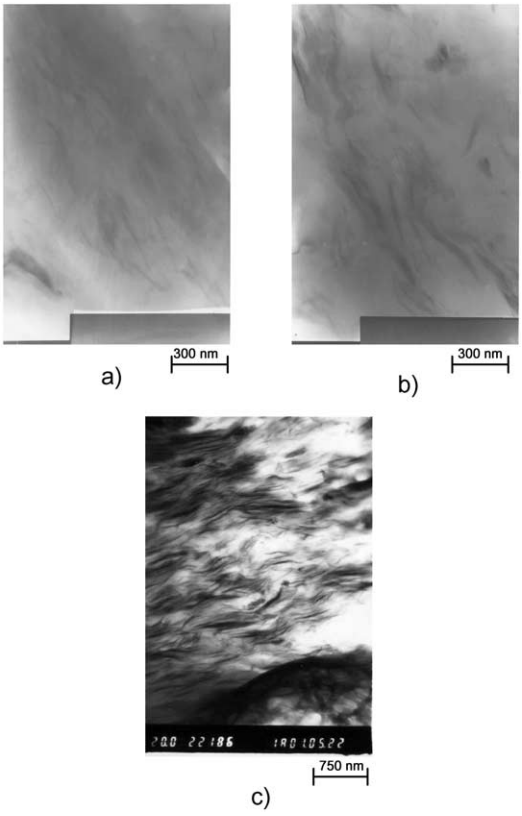

Fig. 5. TEM images of APES/Cloisite 30B hybrids of different contents of clay: (a) 5 wt%, (b) 10 wt% (×150K), (c) 10 wt% (×20K).

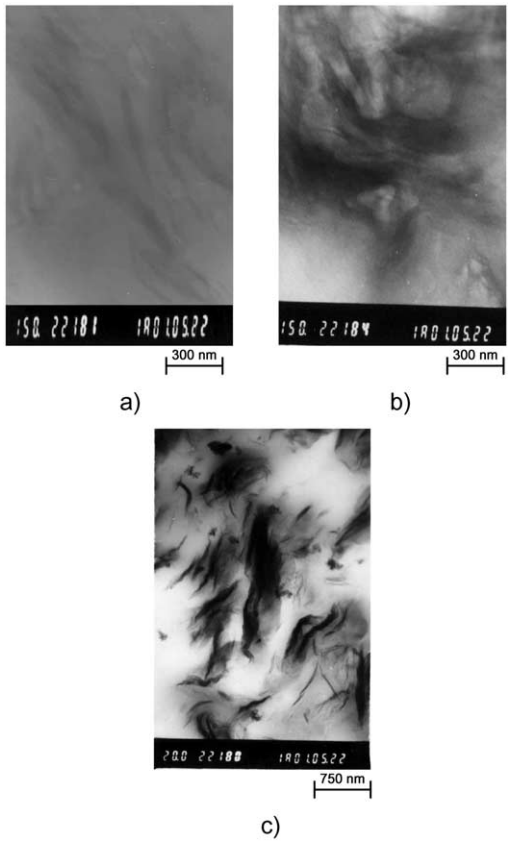

Fig. 6. TEM images of TPS/Cloisite 10A hybrids of different contents of clay: (a) 5 wt%, (b) 10 wt% (×150K), (c) 10 wt% (×20K).

The TEM images of APES/Cloisite 30B hybrids showed intercalated nanostructrures with an expanded layer gap (Fig. 5a and b), regardless of the clay contents. The APES/Cloisite 30B hybrid with 10 wt% of Cloisite 30B shows good dispersion and ordered intercalated structure. From the TEM images of APES/Cloisite 10A hybrids one can see the layered structures of the organoclays though a few aggregated particles remained, indicating the lack of compatibility between APES and the Cloisite 10A. If the clay content is over 10 wt%, the dispersion of clays in the APES matrix becomes slightly worse for the Closite 10A hybrid systems.

3.2. Mechanical properties of the nanocomposites

The tensile properties of APES/Cloisite 30B and APES/Cloisite 10A hybrids at various content of Cloisite 30B and Cloisite 10A are shown in Tables 1 and 2, respectively. In comparison to the APES, the tensile strength and modulus have been improved with little decrease of elongation at break. APES/Cloisite 30B hybrids exhibit higher tensile strength and modulus than the APES/Cloisite 10A hybrids, especially at high organoclay contents. This is also attributed to the strong hydrogen bonding between APES and Cloisite 30B, and further confirms the importance of the strong interaction between the polymer and the organoclay in the formation of nanocomposites with better dispersion as already seen in the TEM and XRD results. In Table 2, the lower tensile strength of the APES/Cloisite 10A hybrid of 70/30 compositions than any other hybrids may be due to the poor dispersion of the clay aggregates in the APES matrix.

Table 1
Tensile properties of APES/Cloisite 30B hybrids

Content of Cloisite 30B (wt%)	Tensile strength (Kgf/cm^2)	Elongation at break (%)	Tensile modulus (Kgf/cm^2)
0	131.7	12.45	106.7
1	139.0	12.25	112.3
3	144.1	11.95	114.4
5	149.8	11.40	118.2
10	157.7	10.90	129.5
20	190.8	11.30	144.4
30	213.5	12.25	173.8

Table 2
Tensile properties of APES/Cloisite 10A hybrids

Content of Cloisite 10A (wt%)	Tensile strength (Kgf/cm^2)	Elongation at break (%)	Tensile Modulus (Kgf/cm^2)
0	131.7	12.45	106.7
1	137.6	12.00	110.3
3	140.2	12.15	115.2
5	145.2	13.05	117.3
10	159.8	11.99	118.9
20	152.7	12.30	120.5
30	132.7	12.30	122.1

3.3. Biodegradability of the nanocomposites

As far as we know, only one paper reported some results about the biodegradability of polymer/clay nanocomposites based on poly (ϵ-caprolactone) (PCL) and organoclays [10], where the authors found that the PCL/clay nanocomposites showed improved biodegradability compared to pure PCL due to the catalytic role of the clay in the biodegradation mechanism. But it is unclear how the clay increases the biodegradation rate of the PCL.

Different results were obtained in our research that the biodegradability of APES/organic MMT nanocomposites decreased with increasing the amount of organoclays except the APES/Cloisite 10A (70/30) hybrid, as shown in Figs. 7 and 8. Comparing Fig. 7 with Fig. 8, one can also see that the APES/Cloisite 10A hybrids exhibit higher biodegradability than the APES/Cloisite 30B hybrids.

The lowering of the biodegradability of APES/organic MMT nanocomposites may come from the presence of dispersed silicate layers with large aspect ratio in the APES matrix, which force the microorganism diffusing in the bulk of the film through more tortuous paths. Therefore the effective path length and time for the microorganism diffusion were increased and the biodegradation of the APES hindered. As mentioned above, APES/Cloisite 30B hybrids showed higher degree of intercalation of organoclays in the APES matrix. Thus, it may be even more difficult for the microorganism to traverse the APES/Cloisite 30B hybrid films, thus their biodegradability is lower than APES/Cloisite 10A hybrids.

The presence of dispersed large aspect ratio silicate layers in the polymer matrix will improve the barrier properties of the nanocomposites at the same time. This is very important to the APES and its composites for use in food packaging, protective coating and so on. On the other hand, the deceased permeability may also relate to the decrease of the biodegradability [9]. For example, if the water permeability in the biodegradable polymer composite films is reduced, the degradation rate may decrease because the hydrolysis of the matrix polymer is likely to depend on the transport of water from the surface into the bulk of the film. This will be the objective of our further research. What we should remember and is of great importance is through preparing polymer/clay hybrids with desired morphology to be able to improve the mechanical properties, the barrier property, and even thermal property with acceptable biodegradation rate.

4. Conclusions

Biodegradable APES/organoclay nanocomposites were

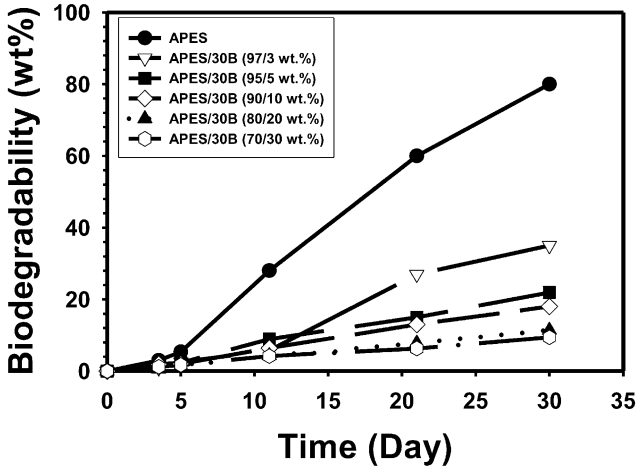

Fig. 7. Biodegradability of APES/Cloisite 30B nanocomposites with different contents of Cloisite 30B.

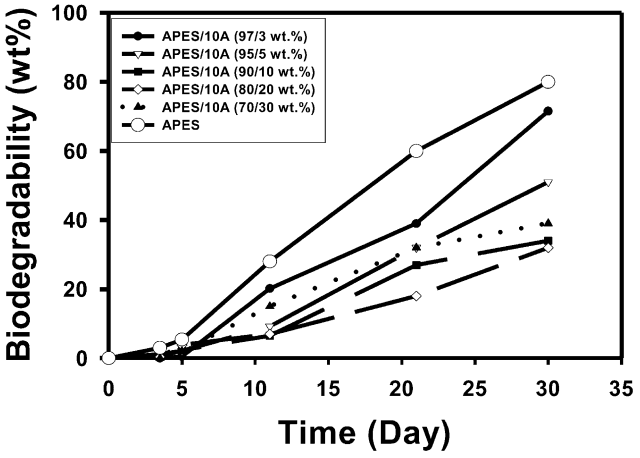

Fig. 8. Biodegradability of APES/Cloisite 10A nanocomposites with different contents of Cloisite 10A.

prepared through melt mixing of APES with two kinds of organoclays, Cloisite 30B and Cloisite 10A. APES/Cloisite 30B hybrids showed higher degree of intercalation than APES/Cloisite 10A hybrids do due to the strong hydrogen bonding interaction between APES and hydroxyl group in the gallery of Cloisite 30B silicate layers. This leads to higher tensile properties and lower biodegradability for APES/Cloisite 30B hybrids than for the APES/Cloisite 10A hybrids. Increasing the content of organoclays in the APES hybrids resulted in high melt viscosity.

Acknowledgements

The work was supported by the Center for Integrated Molecular Systems, POSTECH, Korea and the Brain Korea 21 Project in 2001. The synchrotron XRD measurements were done in the Pohang Accelerator Laboratory, POSTECH, Korea.

References

[1] Lee WK, Doi Y, Ha CS. Macromol Biosci 2001;1:114.
[2] Amass W, Amass A, Tighe B. Polym Int 1989;47:89.
[3] Li X, Kang TK, Cho WJ, Lee JK, Ha CS. Macromol Rapid Commun 2001;22:1310.
[4] Alexandre M, Dubois P. Mater Sci Engng 2000;28:1.
[5] LeBaron PC, Wang Z, Pinnavaia T. J Appl Clay Sci 1999;15:11.
[6] Zanetti M, Lomakin S, Camino G. Macromol Mater Engng 2000;279:1.
[7] Okada A, Usuki A. Mater Sci Engng 1995;C3:109.
[8] Jimenez G, Ogata N, Kawai H, Ogihara T. J Appl Polym Sci 1997;64:2211.
[9] Messersmith PB, Giannelis EP. J Polym Sci, Part A: Polym Chem 1995;33:1047.
[10] Tetto JA, Steeves DM, Welsh EA, Powell BE. ANTEC'99, 1628.
[11] Vaia RA, Giannelis EP. Macromolecules 1997;30:8000.
[12] Kawasumi M, Hasegawa N, Arimitsu M, Okada A. Macromolecules 1997;30:6333.
[13] Ishida H, Campbell S, Blackwell J. Chem Mater 2000;12:1260.
[14] Vaia RA, Jandt KD, Kramer EJ, Giannelis EP. Macromolecules 1997;28:8080.
[15] Tyan HL, Liu YC, Wei KH. Chem Mater 1999;11:1942.
[16] Yoon JT, Jo WH, Lee MS, Ko MB. Polymer 2001;42:329.